# PEROV: R&D for photodetectors based on Organo-Metal Halide Perovskite material

M. Auf der Maur (Ass.), A. De Santis, A. Di Carlo (Ass.), L. Di Marco (Ass.), L. Lo Presti (Ass.), F. Matteocci( Ass.), S. Rizzato (Ass.), S. Sennato (Ass.), M. Testa (Resp.), I. Viola (Ass.), G. Papalino (Tecn.), F. Angeloni (Tecn.)

## 1 Introduction

The organometal halide perovskites (OMHP) semiconductors combine the advantages of organic and inorganic semiconductors. Due to their crystalline structure and band-like electronic properties, they present low exciton binding energy and high charge-carrier mobility. As high Z material, they have a high absorption coefficient that makes a thin layer of material sufficient for almost complete light absorption. The main advantage with respect to the III-V semiconductor technologies is the possibility to scale up over large area substrates by using several printing techniques such as spin and blade coating. These processes typically work at low temperatures and under ambient conditions and allow to fabricate thin film devices on large areas of several square centimeters. Therefore they are attractive to build large area photodetectors with possibility for curved shapes. OMHP can also be grown in large and highquality single crystals with seeding techniques or with unconventional lithographic techniques (such as soft-lithography, microfluidics or dewetting-driven deposition).These latter offer less scalability as printing techniques, but provide higher purity which, depending on the application context, may be of higher priority.

A prerequisite to use OMHP semiconductors to detect low intensity signals is the presence of a gain. This latter has been described in literature in association with a slow time response, related to the presence of traps in the OMHP film. The main goal of the PEROV project is to find out whether OMHPs exhibit also fast internal avalanche multiplication. The second goal is to study the stability of perovskite devices.

## 2 Device production and characterization

In the PEROV project three classes of devices have been realized through a dedicated optimization of the perovskite-crystal growth. Xray diffraction and Scanning Electron Microscopy have been used to measure the quality and morphology of the crystals. All the device have been electrically characterized. The perovskite with Bromide has been chosen due to a larger band gap with respect to that with Iodide and due to its larger defect activation energies [3].

1. Production and characterization of film-based device
   Film devices with 300 nm thickness and four 4x4 $mm^2$-area pads were characterized (Fig. 1). Among the produced batches, $\sim$6 devices showed a gain, with an incident photon to current efficiency (IPCE) larger than 100%. Encouragingly, a gain was observed in devices with different transport layers and even without hole transport layer. A rise-time of 2.5 $\mu$s was measured, dominated by transport in the mesoporous $TiO_2$ transport layer. An analytic model including the impact ionization processes and the effect of mobile ions has been implemented in PEROV, Fig. 2, leading to the publication [1].

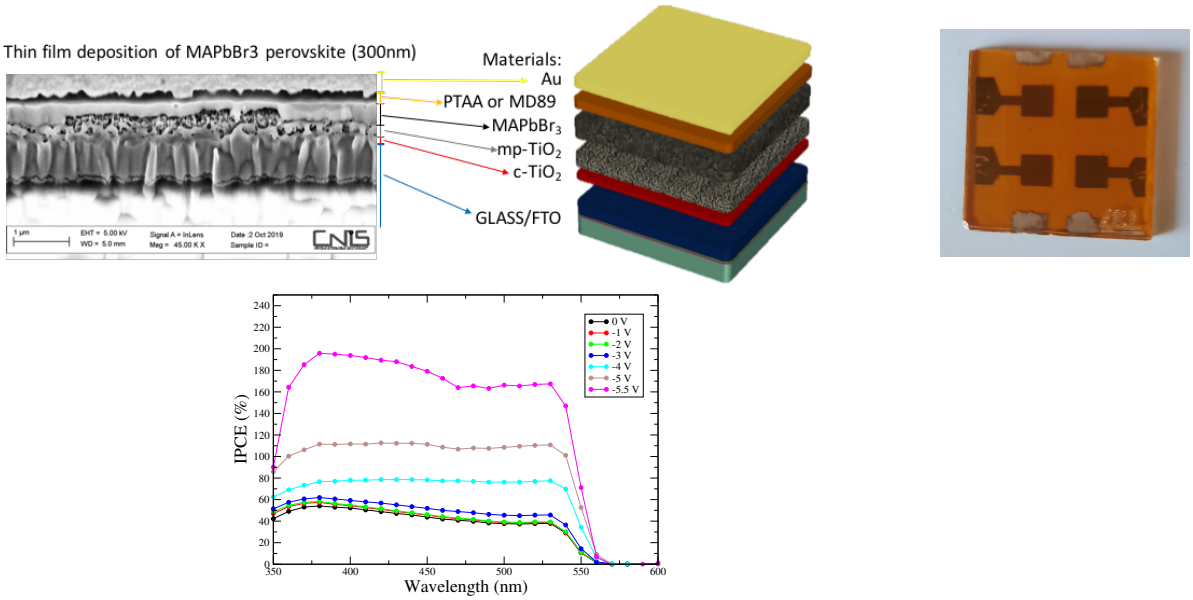


Figure 1: Film characterization. Top Left: Image of scanning electron microscopy and sketch of the device layers. Top Right: film-device. Bottom: incident photon to current efficiency (IPCE) as function of the wavelength at different bias voltage.

2. Micro-fluidics assisted single-crystals production and characterization
   Microwires of $CH_3NH_3PbBr_3$, realized by a microfluidic deposition technique, with total dimensions (W x L x H) of 150 × 250 × 2(6) $\mu m^3$ were deposited. The device is currently subject to a patent submission [2)] and details can not be yet published. The devices show an IPCE 3 larger than 100%. The evaporation of the Au contact was possible through 3D printed masks realized by the LNF mechanic workshop.

3. Single crystals production with seeding techniques and characterization (Fig. 4, 5)
   Single crystals with thickness from 300 $\mu$m to 2 mm, with size up to 5×5 $mm^2$ were produced using seeding techniques. The samples were characterized by single crystal X-ray diffraction up to a maximum resolution of 0.7 Å. The prevalent habit is cubic. Symmetry-equivalent {001} facets are exposed, with (101) as possible cleavage directions. The perovskite has the expected Pm-3m symmetry at room temperature. The organic cations occupy the cuboctahedral sites and are orientationally disordered over 48 equivalent sites. Indium tin oxide (ITO) and Au contacts were deposited on the two sides. A resulting device shows an IPCE 5 larger than 100%.

For all the devices the LNF electronic service realized ad-hoc boards for the time-resolved electrical measurements.

## 3 Radiaton hardness

The activity of this WP has been mainly focused on the characterization of the chosen irradiation site: the DAFNE LINAC odoscope, as shown in Fig. 6.

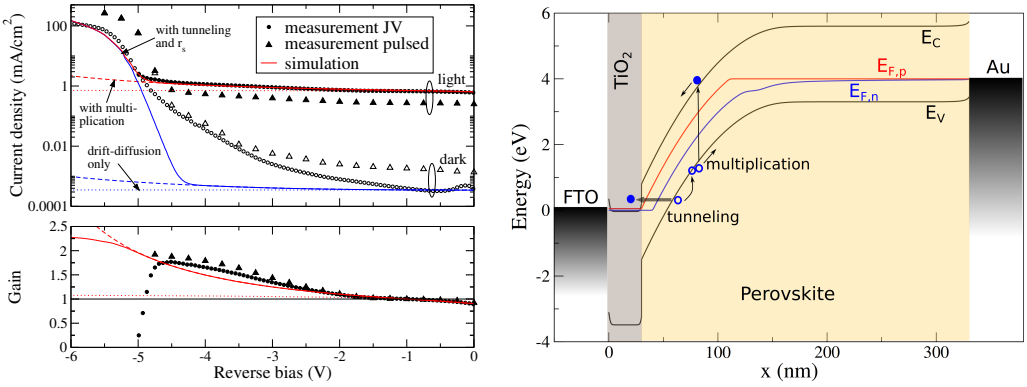


Figure 2: Left: Measured and modeled JV characteristics in dark and under illumination, and gain. The dashed line indicates the dark current without avalanche multiplication. The red solid lines are the currents in dark and under illumination including multiplication. $TiO_2$ doping is $5\times10^{19}$ cm$^{-3}$, and ion concentration is $7.5\times10^{17}$ cm$^{-3}$. Breakdown due to tunneling in this case precedes avalanche breakdown. Right: Band profile at -4 V bias, indicating the high-field region where avalanche multiplication may happen, and band-to-band tunneling through the $TiO_2$/perovskite barrier.

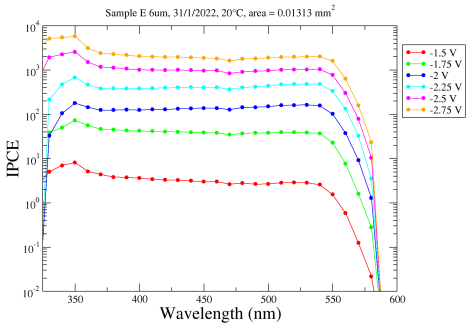


Figure 3: Incident photon to current efficiency (IPCE) of a micro-channel of dimensions (W x L x H) of 150 $\mu$m $\times$ 250 $\mu$m $\times$ 6 $\mu$m

Preliminary measurement and simulations [4], showed the needs of better spatial sampling of the irradiation field. The delivered dose has been mapped in a region of 20x20 cm$^2$ centered on the incoming beam axis, as shown in Fig. 7, right. A reference system has been defined and marked on the surface of the lead shielding wall in order to gran reproducibility of the future irradiation. The application for LINAC odoscope monitoring, embedded in the online DAFNE diagnostics, has been improved, as shown in the Fig. 7-left to grant precise measurements of beam parameters during the planned irradiation runs. Integrated dose measured in December 2021 confirmed the peak value of $\sim$2 mGy/nC delivered dose, showing a reasonable linearity over almost one order of magnitude in terms of delivered beam charge on target. Improved Monte-Carlo simulations are under development in order to verify the dose distribution in both planes. On March, 2022, DAFNE

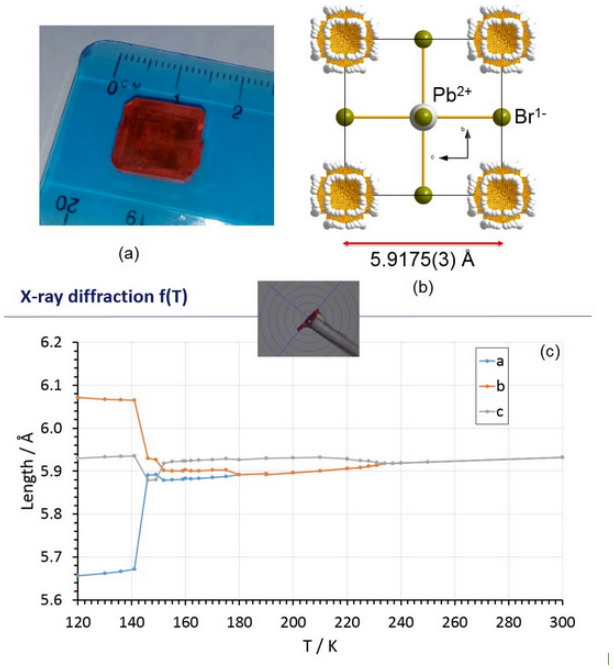


Figure 4: (a) a large single crystal of $CH_3NH_3PbBr_3$ grown from hot DMF solution with the seeding technique. (b) Unit cell content of the cubic phase of $CH_3NH_3PbBr_3$ at RT. The organic cation lies at the vertices of the unit cell and is completely disordered over 48 fully equivalent crystallographic directions. (c) Change of cell edges length as a function of T.

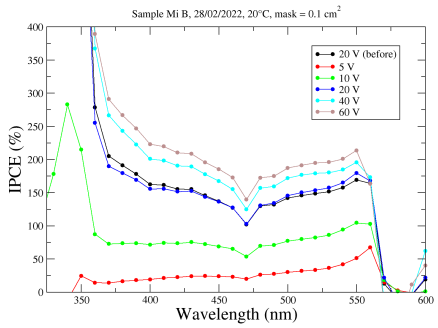


Figure 5: Incident photon to current efficiency (IPCE) of a thick single crystal produced with seeding technique. Measurements using wavelengths below 350 nm are not accurate.

operations were restarted allowing for new measurements and possibly for the first irradiation on a working sample.

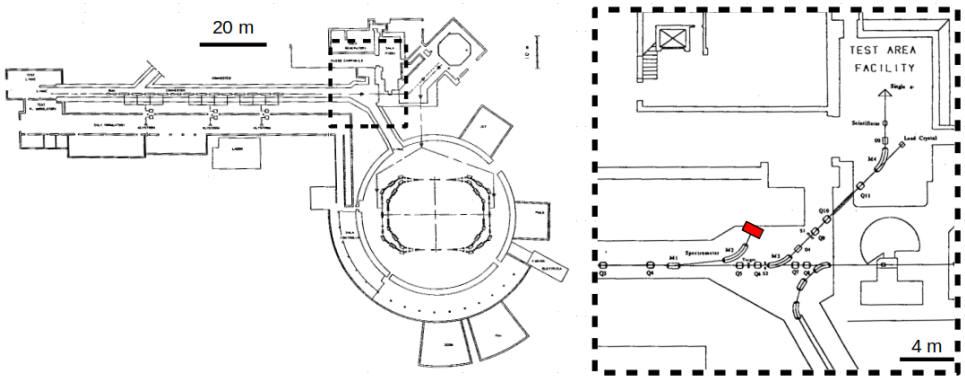


Figure 6: DAFNE complex schematics (left) with the detail (right) of odoscope beamline. The irradiation site is located where the red box is placed, after the beam dump.


Figure 7: Left: Improved Control dashboard realized to monitor the beam parameters distributions (charge and position) while the LINAC is normally operated for injection in the DAFNE Main-Rings. This tool allows online information on the beam spot on the target and thus estimates, on the basis of the calibration, of the expected dose in the irradiation site. Right: radiation field dose map after the odoscope lead shielding. Dose is measured in mGy. (*Data courtesy of LNF radioprotection service*)

## 4 List of Conference Talks by LNF Authors

1. M. Testa on behalf of PEROV coll., Frascati, PEROV: R&D for photo-detectors based on Organo-Metal halide Perovskite material, Workshop Quantum Materials for Quantum Technologies, Laboratori Nazionali di Frascati, February 2022

## 5 Publications

1. Testa M, Auf der Maur M, Matteocci F, Di Carlo A (2022). Reverse bias breakdown and photocurrent gain in CH3NH3PbBr3 films. APPLIED PHYSICS LETTERS, vol. 120, ISSN: 0003-6951, doi: 10.1063/5.0082425

## References

1. Testa M, Auf der Maur M, Matteocci F, Di Carlo A (2022). Reverse bias breakdown and photocurrent gain in CH3NH3PbBr3 films. APPLIED PHYSICS LETTERS, vol. 120, ISSN: 0003-6951, doi: 10.1063/5.0082425

2. On going deposition of patent, Confined growth of perovskite single-crystal on patterned conductive substrate for broad imaging applications , M. Testa, M. Auf der Maur, F. Matteocci, I.Viola, L. Di Marco

3. J. M. Azpiroz et al., Defects Migration in Methylammonium Lead Iodide and their Role in Perovskite Solar Cells Operation, Energy Environ. Sci., 2015,8, 2118-2127

4. M. Testa et al., PEROV: R&D for photodetectors based on Organo-Metal Halide Perovskite material: INFN-CSN5 Activity report July 2021. https://www.ac.infn.it/preventivi/2022/allegati/getfile.php?filename=PEROV_all_2.pdf